Tree Physiology 26, 129–144

DESPOT, a process-based tree growth model that allocates carbon to maximize carbon gain

THOMAS N. BUCKLEY[1–3] and DAVID W. ROBERTS[4]

[1] *Environmental Biology Group and CRC for Greenhouse Accounting, Research School of Biological Sciences, The Australian National University, Canberra, ACT 2601, Australia*

[2] *Present address: Biology Department, Utah State University, Logan, UT 84322, USA*

[3] *Corresponding author (tom_buckley@alumni.jmu.edu)*

[4] *Ecology Department, 310 Lewis Hall, Montana State University, Bozeman, MT 59717, USA*

Received March 15, 2005; accepted July 28, 2005; published online November 8, 2005

Summary We present a new model of tree growth, DESPOT (Deducing Emergent Structure and Physiology Of Trees), in which carbon (C) allocation is adjusted in each time step to maximize whole-tree net C gain in the next time step. Carbon gain, respiration and the acquisition and transport of substitutable photosynthetic resources (nitrogen, water and light) are modeled on a process basis. The current form of DESPOT simulates a uniform, monospecific, self-thinning stand. This paper describes DESPOT and its general behavior in comparison to published data, and presents an evaluation of the sensitivity of its qualitative predictions by Monte Carlo parameter sensitivity analysis. DESPOT predicts determinate height growth and steady stand-level net primary productivity (NPP), but slow declines in aboveground NPP and leaf area index. Monte Carlo analysis, wherein the model was run repeatedly with randomly different parameter sets, revealed that many parameter sets do not lead to sustainable NPP. Of those that do lead to sustainable growth, the ratios at maturity of net to gross primary productivity and of leaf area to sapwood area are highly conserved.

Keywords: C allocation, forest productivity, optimality, photosynthesis, tree height, water relations.

Introduction

Many topical questions in tree ecophysiology involve structural and functional adaptation during growth. Tree growth may usefully be seen as a feedback loop between carbon (C) gain and C allocation: nitrogen (N) and water are captured by roots and transported by stems, light is captured by leaves and all three resources limit photosynthetic carbon gain—N and light constrain the sink strength of the photosynthetic apparatus for CO_2 and water controls the supply of CO_2 through stomatal conductance. Some of the carbon fixed and reduced in leaves is used to augment or replace roots, stems and leaves, shoring up photosynthetic resource capture and delivery and perpetuating the feedback cycle. Tree growth models link the component processes of this feedback loop and are thus powerful tools for understanding its adaptive regulation. When quantitatively accurate growth predictions are desired, empirical modeling is often most appropriate. However, when the aim is to predict growth under novel combinations of environmental conditions (e.g., future climates), or when the object of study is not growth outcomes but the underlying processes and constraints, it is preferable to use more generic and conservative principles.

Process laws are ideal for this purpose because they can be explained in terms of universal physico-chemical principles. Some aspects of tree growth can confidently be modeled on a process basis, including photosynthesis and the capture and delivery of photosynthetic resources. However, the processes that control carbon allocation are not well understood (Le Roux et al. 2001), so another generic principle is needed to simulate allocation. One strong candidate to fulfill this role is adaptation—the tendency for organisms to modify their structure and function in ways that improve performance (and ultimately reproductive success)—which is an embodiment of biology's grand unified theory, natural selection. Teleonomic or goal-directed models attempt to capture adaptation by hypothesizing that, whatever the underlying mechanisms, regulatory processes optimize some quantifiable aspect of organism function. Teleonomic allocation models may even be preferable to process-based models if the aim is to understand the adaptive character of allocation itself and the structural and functional features that emerge from the adaptive regulation of allocation.

Many teleonomic models are based on the assumption that adaptive regulation produces a state of functional balance between plant organs, which is reflected by simple structural patterns (Valentine 1985, Mäkelä 1986, Hilbert and Reynolds 1991, Deleuze and Houllier 1995, Luan et al. 1996, Mäkelä 1997, Grote 1998, Mäkelä 1999, Valentine 1999, Lo et al. 2001, Battaglia et al. 2004). The functional balance paradigm provides convenient and intuitive goal functions that facilitate the analysis of structural features by directing focus toward

costs and benefits that are manifestly relevant to the feature of interest. For example, the ratio of leaf area to sapwood area is often evaluated in terms of hydraulic constraints, with the relevant functional balance being the maintenance of stomatal conductance and leaf water status (Shinozaki et al. 1964*a*, Whitehead et al. 1984, Valentine 1985, Mäkelä 1986, Magnani et al. 2000). This approach offers clarity and simplicity. It also has the advantage of creating analytical constraints—generic mathematical relationships that summarize, in a highly accessible form, what is known about conserved features of structural adaptation. Mathematical simplicity is a prerequisite for the incorporation of such powerful knowledge into predictive models, so its importance cannot be overstated.

However, the functional balance approach has some limitations and drawbacks. An analysis that focuses only on the processes that seem relevant may exclude other processes that significantly impact the costs and benefits of the feature in question if those impacts are sufficiently subtle or indirect to elude intuition. For example, C gain can be largely decoupled from the dynamics of any single resource because photosynthesis is limited by several substitutable resources (Mooney et al. 1978, Field et al. 1983, Reich et al. 1989, Cordell et al. 1999, Miller et al. 2001). This means that all functional C pools are economically interwoven: a change in allocation to one pool affects every other, and not only by mass balance, but also by changing the costs and benefits associated with allocation to those other pools. Replacing C gain by the more restrictive proxy goal of some particular functional balance precludes the full gamut of resource substitution, thus eliminating an important class of adaptive tactics that real trees may possess. As a result, patterns predicted on the basis of functional balance may not adequately reflect the constraints and opportunities experienced by a growing tree.

For these reasons, we believe there is merit in creating a model that accounts for the complex economic interdependencies among different C pools and photosynthetic resources by unifying all C allocation decisions under a single goal, and by using numerical optimization to identify growth trajectories that achieve that goal. This reduces the need to assume that certain tradeoffs are irrelevant to the feature of interest. Because it allows most structural features to emerge on their own, it also reduces the need for ad hoc allometric constraints on tree structure. Unlike functional balance, however, this approach is computationally highly intensive, so it is unlikely to yield mathematically simple predictions and it is unsuitable for use in large-scale predictive modeling. Its role, instead, is to clarify and improve the theoretical basis of simpler goal-directed approaches, which may then more confidently inform predictive modeling.

This paper presents a model of individual tree growth, DESPOT (Deducing Emergent Structure and Physiology Of Trees), that treats structural adaptation during growth as an optimization process in which the central currency is reduced C, the control parameters are C allocation fractions, the goal is to maximize growth (or, equivalently, net structural C gain or single-tree net primary production) and the underlying cost-benefit structure is implicit in a suite of process models for photosynthesis and for the acquisition and transport of substitutable photosynthetic resources (N, light and transpirable water). Constraints on structural geometry due to windthrow risk are treated with a mechanical and probabilistic approach. In this paper, we describe the general behavior of DESPOT, compare it with published data and evaluate the extent to which the model's predictions are qualitatively robust by Monte Carlo parameter sensitivity analysis. The model itself is described in the Appendix. An accompanying paper (Buckley and Roberts 2006) discusses the model's predictions for hydraulic compensation during height (H) growth.

Overview of model assumptions

For ease of reference, the model's structure and core assumptions are summarized below. The reader is directed to the Appendix for more details.

Carbon allocation

In each time step, the total C increment available for structural growth is allocated to leaves, fine roots and radial, aboveground axial (height) and belowground axial (depth) sapwood production. A numerical algorithm finds the allocation fractions that maximize the C increment in the next time step.

Carbon gain

Photosynthesis is calculated with a big-leaf version of the Farquhar et al. (1980) photosynthesis model, based on electron transport and carboxylation capacities, photosynthetic irradiance and stomatal conductance.

Nitrogen

Photosynthetic capacity parameters are proportional to leaf N content, and canopy N content is simulated dynamically based on the balance between uptake by fine roots, losses due to senescence and N requirements for new increments of non-photosynthetic tissues with fixed C:N ratios. Soil N input is a fixed parameter.

Light

Leaf-level irradiance is a canopy average based on total light capture, which is calculated by Beer's Law. The marginal response of canopy light capture to H growth is calculated explicitly, assuming each canopy is rectangular in cross section and the stand is closed.

Water

Stomatal conductance is proportional to transpiration rate by a constant evaporative gradient. Canopy transpiration rate is assumed to be in steady-state with water movement from the soil to the site of evaporation, which in turn is calculated from Darcy's Law. Independent resistance terms are used to describe the effects of fine roots, axial flow path length and sapwood area. The hydraulic gradient driving this flow is constrained by assuming fixed soil and leaf water potentials.

However, in the accompanying paper (Buckley and Roberts 2006), simulations are also performed in which leaf water potential declines enough to offset the *H*-related gravitational head.

Carbon balance

Senescence is modeled by tracking each individual increment of leaf, fine root and sapwood C and decrementing these increments over time based on the assumption of a Weibull distribution of tissue lifespans. Maintenance respiration is calculated independently for each C pool in fixed proportion to its N content; construction respiration is a fixed fraction of gross C gain minus respiration.

Miscellaneous

Most parameters were estimated to represent lodgepole pine (*Pinus contorta* Dougl. ex. Loud.). Windthrow risk, which is used to depress the apparent profitability of mechanically risky candidate allocation vectors, is estimated from canopy sail area, basal trunk diameter and coarse root anchorage depth, using a highly simplified mechanical model. Branching and tapering are not explicitly described. Instead, radial and axial sapwood increments are computed from their respective allocation fractions and the total wood C increment based on an empirical relationship between total stemwood volume (including branches) and radial and axial stem dimensions. This relationship, which implicitly captures aboveground branching and tapering patterns, is assumed to hold for coarse roots. The available ground area per tree and aspects of canopy geometry needed to estimate the benefit of *H* growth are simulated by assuming the stand is uniform, and that it self-thins according to the –3/2 power law. All processes are simulated on an annual basis, so diurnal and seasonal effects such as temperature variation are ignored.

Results and discussion

General behavior of the model

Variables in the model are presented in Table 1. The simulations described here and illustrated in Figures 1 and 2 used parameter values estimated for lodgepole pine and, where possible, specifically for the lodgepole chronosequence studied by Ryan and Waring (1992) (Table 2). Therefore, comparable data from that chronosequence are shown with symbols in Figures 1 and 2, and Table 3 summarizes the comparison in tabulated format.

Despite the minimal degree to which C partitioning and *H* growth are empirically constrained in the model, DESPOT predicts growth trajectories that compare fairly well with the observations of Ryan and Waring (1992) for 40- and 65-year-old lodgepole pine stands. In both the model and the data, leaf area index (LAI) increases quickly to around 10–12, and net and gross primary productivity (NPP and GPP, respectively) also peak by 40 years (at about 0.5 and 0.9 kg C m^{-2} $year^{-1}$, respectively), whereas *H* increases more steadily to around 10 m at 40 years, and around 12 m at 65 years (Figure 1, Table 3). However, *H* growth in DESPOT tapers off at around 75 years and both NPP and GPP remain nearly constant. In contrast, Ryan and Waring (1992) found a further 45% increase in *H* from 65 to 245 years, together with declines of 47 and 37%, respectively, in NPP and GPP (Figures 1a and 1c, Table 3). Many other data confirm that aboveground NPP (ANPP) generally declines with age in forest stands (see review by Ryan et al. 1997). DESPOT predicts a moderate de-

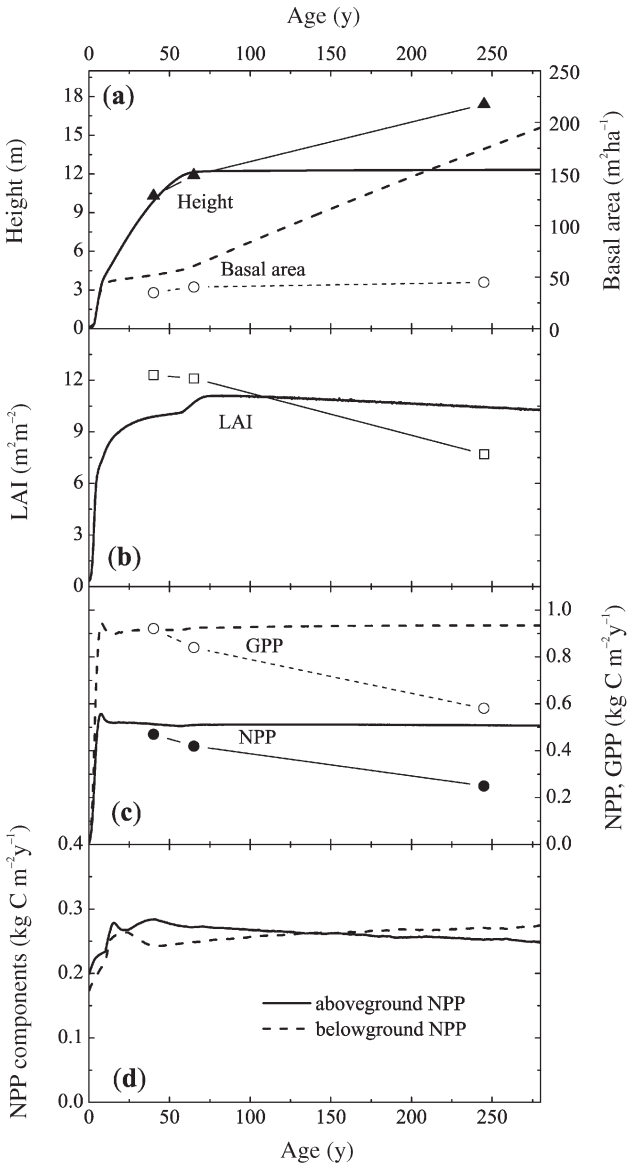

Figure 1. Time courses of major tree and stand growth variables predicted by DESPOT for the parameter values given in Table 1 (thick lines), compared with analogous data (symbols connected by thin lines) observed by Ryan and Waring (1992) for a lodgepole pine chronosequence in Colorado, USA. (a) Height (solid lines and closed symbols) and basal area (broken lines and open symbols); (b) leaf area index (LAI); (c) gross primary productivity (GPP, broken lines and open symbols) and net primary productivity (NPP, solid lines and closed symbols); (d) above- and belowground NPP (ANPP, BNPP; solid and broken lines, respectively).

Table 1. Variables in DESPOT. "minh{*a,b,c*}" means "the lesser root Q of $cQ^2 - (a + b)Q + ab = 0$." Subscripts for allocation fractions and carbon (C) pools are: l = leaves; r = fine roots; sw = sapwood; hw = heartwood; w = total wood; t = total C (sum of all pools); d = radial sw allocation; h = aboveground axial sw allocation; z = belowground axial sw allocation; and N = nitrogen.

Variable	Symbol	Units	Equation
Allocation fractions (x = l,r,d,h,z)	a_x	unitless	1
Leaf net CO_2 assimilation rate	A	μmol C m^{-2} s^{-1}	6
A when RuBP carboxylation is limiting	A_c	μmol C m^{-2} s^{-1}	5
A when RuBP regeneration is limiting	A_r	μmol C m^{-2} s^{-1}	5
Supply equation for A	A_s	μmol C m^{-2} s^{-1}	5
Single tree net primary production	A_n	mol C $year^{-1}$	2
Single tree gross primary production	A_t	mol C $year^{-1}$	3
Canopy "absorptance"	α_c	unitless	10–12
Intercellular CO_2 mole fraction	c_i	μmol CO_2 mol^{-1}	5, 6
Carbon pools (x = l,r,sw,hw,w,t)	C_x	mol C	–
Basal trunk diameter	D_b	m	–
Leaf-level transpiration rate	E	mmol H_2O m^{-2} s^{-1}	$E_t/L \cdot 10^3$
Whole-tree transpiration rate	E_t	mol H_2O s^{-1}	7
Total leaf conductance to CO_2	g_{tc}	mol m^{-2} s^{-1}	$g_s/(1.6 + 1.37 r_{bw} g_s)$
Stomatal conductance to H_2O	g_s	mol m^{-2} s^{-1}	$E/(D - r_{bw}E)$
Canopy projected ground area of one tree	G	m^2	$1/\rho_s$
Stand-level gross primary productivity	GPP	kg C m^{-2} $year^{-1}$	$0.012 \cdot \rho_s A_t$
Vertical span of axial flow path length	h	m	$H(1 - 0.5\ \mathrm{LCR}) + Z/\sqrt{2}$
Tree height	H	m	–
Leaf-level incident irradiance	I	μmol m^{-2} s^{-1}	I_t/L
Whole-tree light capture	I_t	μmol s^{-1}	10–12
Potential electron transport rate	J	μmol e^- m^{-2} s^{-1}	$\mathrm{minh}\{J_m, \phi I, \theta_J\}$
Electron transport capacity	J_m	μmol e^- m^{-2} s^{-1}	$\chi_j N$
Leaf-specific hydraulic conductance	K_L	mmol H_2O $m^{-2} s^{-1} MPa^{-1}$	$E/\Delta P$
Axial flow path length	l	m	Text after 7
Leaf area, projected leaf area	L, L_p	m^2	$\mathrm{SLA} \cdot C_l$, $L/3.34$
Stand-level leaf area index	LAI	m^2 m^{-2}	$\rho_s L_p$
Leaf photosynthetic N content	N	mmol N m^{-2}	N_t/L
Stand-level net primary productivity	NPP	kg C m^{-2} $year^{-1}$	$0.012 \cdot \rho_s A_n$
Canopy photosynthetic N content	N_t	mmol N	8, 9
Pressure gradient from soil to leaf	ΔP	MPa	7
Probability of stem breakage	p_b	unitless	24
Probability of uprooting	p_u	unitless	24
Canopy laminar resistance	r_l	(mol H_2O)$^{-1}$ s MPa	r_{la}/L
Soil–xylem hydraulic resistance	r_s	(mol H_2O)$^{-1}$ s MPa	7
Axial (xylem) hydraulic resistance	r_x	(mol H_2O)$^{-1}$ s MPa	7
Leaf respiration in the day	R_l	μmol CO_2 m^{-2} s^{-1}	$0.01 \cdot V_m$
Maintenance respiration	R_m	mol C $year^{-1}$	2
Stand density	ρ_s	trees m^{-2}	21
Sapwood area	S	m^2	20
Maximum RuBP carboxylation velocity	V_m	μmol CO_2 m^{-2} s^{-1}	$J_m/2.1$
Crown width	W	m	$G^{1/2}$ $(=1/\rho_s^{1/2})$
Rooting depth	Z	m	–

cline in ANPP of around 15% from 50 to 250 years, but this is countered by an increase in belowground NPP (BNPP) (Figure 1d) driven by changes in windthrow risk.

Windthrow risk

One emergent feature of the growth trajectories predicted by DESPOT is a balance between the probabilities of windthrow due to stem breakage and uprooting (p_b and p_u, respectively). The model chooses allocation fractions that maximize the product of net C gain with the complement of the greater of p_b and p_u (see Appendix for details), so these probabilities can be thought of as a risk tax to discourage the production of mechanically untenable growth forms, such as excessively top-heavy or tall and thin trunks. Figure 2 shows that p_b and p_u increase rapidly and in concert during early H growth, causing the risk tax to exceed 14%. Height growth then slows as its perceived benefit for light competition declines as a result of stand thinning and as its hydraulic costs increase. The risk tax then declines until H growth ceases. The risk of stem breakage continues to decline because its dependence on the third power

Table 2. Parameters in DESPOT. Source notations are as follows: (1) de Pury et al. (1997); (2) Ryan and Waring (1992); (3) Murty et al. (1996); (4) Whitehead et al. (1984); (5) observations by the authors; (6) Ryan (1991); (7) Dewar and McMurtrie (1996); (8) Ryan (1989); (9) Yoder et al. (1994); (10) Dougherty et al. (2003); (*) see details in *Parameter estimation* in Appendix; and (†) assumption.

Parameter	Symbol	Value	Units	Source
Effective solar angle (zenith = 0°)	β	54.5	degrees	*
Ambient CO_2 mole fraction	c_a	370	μmol CO_2 mol^{-1}	†
Nitrogen cost of electron transport capacity	χ_j	1.9	μmol e^- s^{-1} $(mmol\ N)^{-1}$	1
Leaf-to-air water vapor mole fraction gradient	D	0.015	mol H_2O mol^{-1}	†
Weibull parameter for senescence failure rates	ε	4	unitless	†
Quantum yield of electrons from incident irradiance	ϕ	0.3	e^- $photon^{-1}$	†
Construction respiration fraction	f_c	0.22	unitless	2
Fraction of N recycled from leaves	γ_l	0.5	unitless	3
Fraction of N recycled from sapwood	γ_{sw}	0.6	unitless	3
Photorespiratory compensation point	Γ_*	37	μmol CO_2 mol^{-1}	1
Solar beam irradiance	I_s	1915	μmol m^{-2} s^{-1}	*
Fine root C per unit ground area at half max N uptake	κ	16.0	mol C m^{-2}	*
Light extinction coefficient	k_L	0.5	m^2 m^{-2}	3
Soil–xylem hydraulic conductance per mol fine root C	k_{ue}	8.3×10^{-4}	mol H_2O $MPa^{-1}s^{-1}(mol\ C)^{-1}$	*
Sapwood permeability	k_s	2.05×10^{-12}	m^2	4
Effective Michaelis constant for Rubisco	K'	746	μmol CO_2 mol^{-1}	1
Live crown ratio	LCR	0.84	unitless	5
Leaf and fine root maintenance respiration per unit N	ν	0.041	mol C $year^{-1}$ $(mmol\ N)^{-1}$	6
Nitrogen content of fine roots	n_r	17	mmol N $(mol\ C)^{-1}$	7
Nitrogen content of sapwood	n_{sw}	1.2	mmol N $(mol\ C)^{-1}$	3
Colimitation parameter for photosynthesis	θ_A	0.9	unitless	†
Colimitation parameters for potential e^- transport	θ_J	0.9	unitless	†
Boundary layer resistance to water vapor	r_{bw}	0.5	m^2 s mol^{-1}	†
Leaf laminar resistance parameter	r_{la}	60	MPa s $(mol\ H_2O)^{-1}$	*
Wood carbon density	ρ_{cw}	1.4×10^4	mol C m^{-3}	8
Self-thinning parameter	ρ_{sc}	49	trees m^{-2} $(mol\ C)^{2/3}$	2
Initial stand density	ρ_{si}	5	trees m^{-2}	†
Leaf area per unit C	SLA	0.091	m^2 $(mol\ C)^{-1}$	3
Median leaf lifespan	τ_l	8.3	year	3
Median fine root lifespan	τ_r	1.0	year	3
Median sapwood lifespan	τ_{sw}	14	year	5
Total N input per unit ground area	U_o	660	mmol N $year^{-1}$ m^{-2}	*
Extreme value index for windspeeds	ω	–0.25	unitless	10
Windthrow risk parameter for stem breakage	w_b	1.15×10^5	unitless	*
Windthrow risk parameter for uprooting	w_u	2.3	m^{-1}	*
Parameter relating trunk dimensions to volume	ξ	0.299	m^3 m^{-3}	*
Time integration factor	Y	3.1	mol $year^{-1}$ $(\mu mol\ s^{-1})^{-1}$	*
Leaf water potential	ψ_l	–1.5	MPa	9
Soil water potential	ψ_s	–0.5	MPa	9

of basal trunk diameter (D_b; Equation A22) allows the stem's bending resistance to outpace the increase in turning moment caused by increasing canopy sail area, which results from stand thinning. However, the uprooting risk continues to increase because the costs of mitigating that risk by axial growth of woody roots, such as hydraulic path length, sapwood respiration and diversion of C from other pools, are too large to justify total mitigation of uprooting risk.

Broad-spectrum parameter sensitivity analysis

It was not our intention to produce a model for lodgepole pine, but instead to create a generic theoretical structure for studying tree growth. Therefore, to determine how qualitatively robust DESPOT's general behavior is, we performed a broad-spectrum Monte Carlo parameter sensitivity analysis in which all parameters were varied randomly by ± 25% of the standard values given in Table 2 (except for live crown ratio, (LCR), which was capped at 1.0), among 100 simulations, each 200 years in length.

The numerical values predicted at 200 years for most major tree and stand variables, such as tree H, LAI, NPP and GPP, varied widely among simulations. For example, H at 200 years ranged from 0.5 to 45 m; NPP ranged from zero to 0.82 kg C m^{-2} $year^{-1}$; and all-sides LAI ranged from zero to 15.7. However, several qualitative results were conserved among parameter sets. In 52 of 100 simulations, NPP had declined to zero by 200 years, but in other simulations productivity achieved a sustainable maximum. In all simulations, H growth eventually

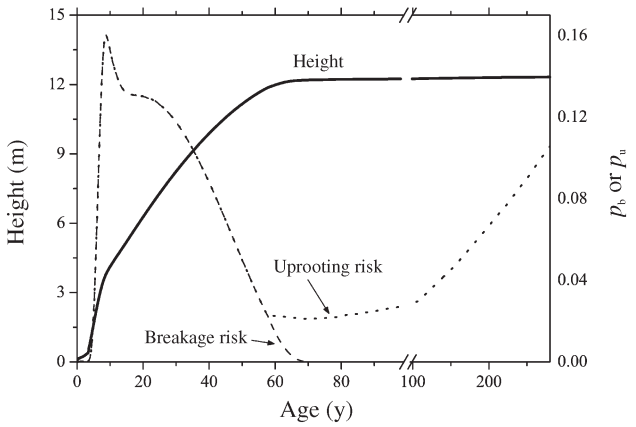

Figure 2. Time courses of height (solid line) and windthrow risk (p_u (dotted line) = probability of uprooting; and p_b (dashed line) = probability of stem breakage) during height growth, predicted by DESPOT for the parameters values given in Table 1. Structural regulation by DESPOT balanced the probabilities of uprooting and breakage, so that they were nearly equal until an age of approximately 60 years. Note the axis break and change of scale at 100 years.

ceased and both intercellular CO_2 mole fraction (c_i) and stomatal conductance (g_s) declined during H growth.

At 200 years, NPP and GPP were linearly correlated with a slope of 0.495 (Figure 3a), which is fairly close to the value (0.47) found by Waring et al. (1998) for a range of species. Dewar et al. (1999) showed that strong conservation in the ratio of NPP/GPP could be explained by substrate limitation for respiration. However, DESPOT predicts that a similar relationship should emerge even when respiratory coefficients (maintenance respiration per unit tissue N, (v), and construction respiration fraction, (f_c)) vary randomly among simulated trees, which suggests that the adaptive regulation of C allocation may also be partly responsible for this conserved emergent property of tree physiology.

Sapwood area and projected leaf area (S (cm^2) and L (m^2), respectively) at 200 years were also linearly correlated among parameter sets, with the best fit provided by a power law with an exponent close to unity: $L = 0.238S^{0.9995}$ (Figure 3b). This is similar to the slope of 0.23 found by Whitehead et al. (1984) for lodgepole pine, but higher than some other values: cf. 0.19 (Dean and Long 1986), 0.13 (Kaufmann and Troendle 1981), 0.06–0.17 (Pearson et al. 1984) (values from the latter two references were divided by 3.34 to estimate projected area).

Summary of predictions

Several of the model's qualitative predictions seem intuitive, but many others are either non-intuitive or manifestly inaccurate. In the hope of promoting discussion or experimentation to improve our understanding of the goals and constraints that shape tree growth and thus also to improve the logical structure of DESPOT, Table 4 summarizes some of the model's salient predictions (several of these predictions are drawn from simulations described in the accompanying paper, Buckley and Roberts 2006). The predictions are labeled by the degree to which they seem intuitive (based on our own opinions and on discussions with colleagues) and by the degree to which they are accurate (if known or applicable). The most significant predictions that are either inaccurate or counterintuitive are: (1) that NPP reaches a sustainable maximum and does not subsequently decline; (2) that H growth ceases at around the same time that NPP stabilizes; (3) that the ratio of L/S declines with H during most of H growth; and (4) that arbitrary reductions in the accuracy or precision of the model's optimization algorithm cause sustained H growth. (The latter two predictions are from Buckley and Roberts 2006.)

The accompanying paper (Buckley and Roberts 2006) discusses possible explanations for divergence of DESPOT's qualitative predictions from observations. Two of these possibilities seem most likely to explain why the model fails to predict indefinite H growth and declining productivity: failure of the assumption that the processes controlling C allocation in real trees achieve the precise numerical optima identified by our computer simulations and failure of the assumption that the goal of C allocation is always and simply to maximize C gain.

Why is DESPOT novel?

Our model is novel in its synthesis of three major features: (1) the teleonomic goal (to maximize C gain); (2) a comprehensive cost-benefit structure for C gain based on process models for photosynthesis and for the delivery of three major substitutable photosynthetic resources, plus an economic treatment of windthrow risk; and (3) the lack of prescribed relationships between emergent structural or physiological

Table 3. Comparison between DESPOT predictions and observations (RW) by Ryan and Waring (1992) of a lodgepole chronosequence in Colorado. Abbreviations: LAI = leaf area index; NPP = net primary productivity; GPP = gross primary productivity; and C = carbon.

Quantity	Age (year)	Height (m)	Basal area (m^2 ha^{-1}) $year^{-1}$)	LAI (kg C m^{-2}	NPP (kg C m^{-2} $year^{-1}$)	GPP (kg C m^{-2})	Total biomass C (kg C m^{-2})	Stand density (stems ha^{-1})
DESPOT	40	9.9	52.5	9.9	0.51	0.92	4.8	7171
	65	12.1	60.9	10.7	0.51	0.92	6.9	3583
	245	12.3	174.3	10.4	0.51	0.93	20.5	405
RW	40	10.3	35.2	12.3	0.47	0.92	6.2	4367
	65	11.9	40.4	12.1	0.42	0.84	7.6	3311
	245	17.4	44.7	7.7	0.25	0.58	9.0	1067

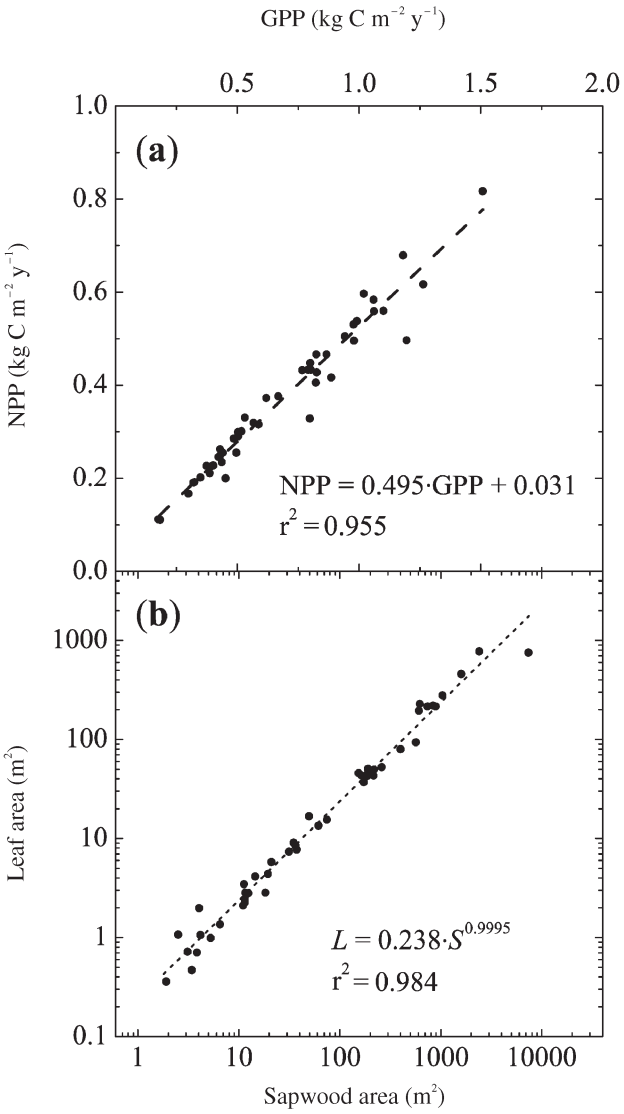

Figure 3. Two generic relationships that emerged from broad-spectrum Monte Carlo parameter sensitivity analysis, in which every parameter in Table 2 was varied randomly within a uniform distribution ranging between 75% and 125% of the value given in Table 2 (except live crown ratio (LCR), which was capped at 1.0), in 100 different simulations. Each value represents a different parameter set and hence a different simulated tree and environment, sampled at an age of 200 years. Cases where NPP (net primary productivity) was less than 0.01 kg C m^{-2} year^{-1} at 200 years are not shown. (a) GPP (gross primary productivity) vs. NPP (the broken line is a linear regression with equation NPP = 0.495·GPP + 0.031 and r^2 = 0.955) and (b) leaf area (L) vs. sapwood area (S) (the broken line is a power function fitted to the values shown, with equation $L = 0.238 \cdot S^{0.9995}$ and r^2 = 0.984).

dimensions. We are unaware of any model that includes all of these features.

Some growth models predict C allocation based on empirical allocation fractions (e.g., G'DAY, Comins and McMurtrie 1993) or a hierarchy of sink priorities (e.g., FOREST-BGC, Running and Coughlan 1988, TREGRO, Weinstein et al. 1991). Many other models are teleonomic—they assume allocation is regulated to achieve some goal—but the specified goal varies widely among models. For example, the WBE model (West et al. 1999) supposes that the goal of biomass partitioning is to minimize hydraulic resistance per unit of light-capturing leaf area and King (1990, 1993) evaluated H growth with respect to the goal of maximizing wood production.

Several teleonomic models assume, like DESPOT, that the goal of C allocation is to maximize C gain or growth (e.g., Reynolds and Thornley 1982, Johnson and Thornley 1987, Hari et al. 1990, Hof et al. 1990, Hilbert and Reynolds 1991, Chen and Reynolds 1997). However, none of these models also account for the effects of the three key substitutable resources on photosynthetic C gain. For example, Hilbert and Reynolds (1991) maximized C gain by varying leaf N content using a biochemical model of photosynthesis, but their analysis assumed constant c_i, thus excluding costs and benefits of C allocation for water capture and transport. The model of Hari et al. (1990) explicitly optimized C gain and included responses of photosynthesis to both N and water, but excluded light capture and constrained some aspects of C allocation with an assumption derived from the pipe-model theory. Conversely, of the models that do account for the three substitutable photosynthetic resources, none optimizes C allocation to maximize C gain. (For a comprehensive review of C allocation models, see Le Roux et al. 2001, which lists models according to the methods of simulating C gain and allocation.)

In many other teleonomic models, the goal that drives allocation involves some type of functional balance. Davidson (1969) suggested that plants adjust their root:shoot ratio to balance nutrient uptake rate and C gain and Thornley (1972*a*) showed that this structural balance maximizes growth in a simple model. Although other analyses (Reynolds and Thornley 1982, Mäkelä and Sievanen 1987) have since shown that biomass partitioning must vary over time to maximize growth, the functional balance paradigm persists. There are at least two reasons for this. First, it greatly simplifies modeling—each postulated balance removes at least one degree of freedom from the simulation, because it constrains at least two variables with respect to one another. For example, many models use a constrained relationship between L and S as a convenient way to constrain C allocation (Valentine 1985, Mäkelä 1986, Mäkelä 1999, Valentine 1999, Lo et al. 2001, Battaglia et al. 2004). This is often justified by the pipe-model theory of Shinozaki et al. (1964*a*, 1964*b*), which involves a functional balance between hydraulic supply and demand. Second, there is some mechanistic basis for the functional balance concept. Although the processes controlling C allocation are not well known, evidence suggests C is allocated in proportion to sink strength (Thornley 1972*b*, Dewar et al. 1998, Le Roux et al. 2001). This would yield a homeostatic balance between sink and source strength in the steady state. Similarly, Chen and Reynolds (1997) showed that a model based on dynamic coordination of C and water limitations on growth rate predicted similar, and in some cases identical, growth trajectories as did models based on optimization.

However, functional balance does not necessarily reflect optimal adaptation. Mäkelä (1986) and Valentine (1985) showed

Table 4. Some major qualitative predictions from DESPOT and the degree to which they seem intuitive (to the authors) and accurate. Predictions marked by an asterisk (*) are from simulations described and discussed in the accompanying paper (Buckley and Roberts 2006); of those predictions, the two involving "arbitrary constraints on C allocation" are from simulations in which the accuracy or precision of the allocation optimization algorithm was artificially reduced. For predictions concerning model exercises with no obvious real-world analogue, accuracy is given as "n/a". Abbreviations: H = height; c_i = intercellular CO_2 mole fraction; and g_s = stomatal conductance to water vapor. Abbreviations: NPP = net primary productivity; and GPP = gross primary productivity.

Prediction	Intuitiveness	Accuracy
Productivity		
Ratio of NPP/GPP is somewhat conserved and close to 0.5	Weakly intuitive	Accurate
Ratio of NPP/GPP decreases weakly with increasing H in broad-spectrum Monte Carlo simulation*	Weakly or non-intuitive	Uncertain
NPP reaches sustainable maximum	Nonintuitive	Inaccurate
Arbitrary constraints on C allocation reduce NPP*	Intuitive	n/a
Height growth		
c_i and g_s decline with H during H growth	Intuitive	Usually accurate
Leaf area:sapwood area ratio declines with H during most of H growth*	Counterintuitive	Varies; more often inaccurate
Height growth is clearly determinate	Nonintuitive	Usually inaccurate
Arbitrary constraints on C allocation cause sustained H growth*	Nonintuitive	n/a

that if trees were constrained to obey the pipe-model theory, they would eventually produce pipes that could not pay for their own construction and maintenance costs. Magnani et al. (2000) similarly concluded that the patterns of biomass partitioning dictated by the dual constraints of hydraulic homeostasis and constant stomatal conductance would eventually force aboveground NPP to decline.

What is the point of DESPOT?

The model, DESPOT, is meant to predict emergent qualitative properties of tree structure and function from the hypothesis that C allocation is regulated to maximize C gain, subject to known biophysical constraints on C gain, resource capture, resource transport and mechanical stability. These predictions can improve our understanding of the constraints and goals from which adaptive properties emerge during tree growth. In the accompanying paper (Buckley and Roberts 2006), we begin working toward this end by evaluating possible reasons for qualitative discrepancies between the model's predictions and observations. Analysis of the resource relationships predicted by DESPOT might also prove useful in studying the mechanisms of interspecific competition. For example, the "resource-ratio" theory of Tilman (1980, 1982) suggests that a species' competitive ability is related to its ability to tolerate resource depletion. DESPOT could be used to link familiar tolerance syndromes (e.g., drought tolerance or shade tolerance) to measurable physiological characters. One would construct imaginary species with distinct parameter sets, apply them to DESPOT under varying resource availabilities and catalogue the patterns of tolerance that emerge in the model.

Critically, the model is not meant to be a numerically accurate or predictively useful facsimile of real tree or forest growth. To ensure accuracy by applying ad hoc constraints would be to beg the question by presuming certain outcomes. A more powerful approach is to see what emerges from the optimality hypothesis with minimal constraints and only then to modify the goal and add plausible constraints to bring predictions more in line with observations. In other words, the starting point, or the null hypothesis, should be informed as little as possible by our knowledge or intuition concerning emergent properties of adaptive regulation. "It is not the resemblance between models and reality that lead to new discoveries, but the discrepancies between them" (Pielou 1981) and, "the purpose of models is not to fit the data but to sharpen the questions" (Karlin April 20, 1983; Fisher memorial lecture, Royal Society, London), quoted in Woodward (1987).

Conclusion

The model DESPOT predicts sustained productivity and determinate H growth, but rapid early increases followed by slow declines in both ANPP and LAI. Monte Carlo parameter sensitivity analysis shows that most of these predictions are robust to substantial parameter variation. However, of the 100 parameter sets compared in that analysis, about half led to rapid declines in productivity rather than to sustained growth. In the cases where productivity was sustained, the ratios of NPP to GPP and L to S were somewhat conserved among mature, age-matched simulated trees with different parameter sets. In contrast to DESPOT's predictions, most data show sustained H growth and declining productivity. The accompanying paper (Buckley and Roberts 2006), which uses the model to analyze hydraulic adjustment during H growth in greater detail, discusses possible reasons for these discrepancies.

Acknowledgments

T.N.B. thanks Nathan Phillips and Graham Farquhar for feedback and encouragement; Mike Ryan, Creighton Litton, C.P. Patrick Reid and the USFS Rocky Mountain Research Station Library for providing data to assist with parameter estimation; and Tim Brodribb, David Whitehead, Margaret Barbour, Tom Givnish, Julia Powles, Mike Ryan, Stefan Arndt, Karel Mokany, Mike Roderick and Lawren Sack for helpful input. This work was supported by US National Science Foundation Grant No. 9903947 to DWR, and by the Cooperative Research Centre for Greenhouse Accounting, hosted by the Research School of Biological Sciences at the Australian National University.

References

Battaglia, M., P. Sands, D. White and D. Mummery. 2004. CABALA: a linked carbon, water and nitrogen model of forest growth for silvicultural decision support. For. Ecol. Manage. 193:251–282.

Buckley, T.N. and D.W. Roberts. 2006. How should leaf area, sapwood area and stomatal conductance vary with height to maximize carbon gain? Tree Physiol. 26:145–157.

Chen, J.-L. and J.F. Reynolds. 1997. A coordination model of whole-plant carbon allocation in relation to water stress. Ann. Bot. 80: 45–55.

Comins, H.N. and R.E. McMurtrie. 1993. Long-term biotic response of nutrient-limited forest ecosystems to CO_2-enrichment; equilibrium behavior of integrated plant-soil models. Ecol. Appl. 3: 666–681.

Cordell, S., G. Goldstein, F.C. Meinzer and L.L. Handley. 1999. Allocation of nitrogen and carbon in leaves of *Metrosideros polymorpha* regulates carboxylation capacity and $\delta^{13}C$ along an altitudinal gradient. Funct. Ecol. 13:811–818.

Davidson, R.L. 1969. Effect of root/leaf temperature differentials on root/shoot ratios in some pasture grasses and clover. Ann. Bot. 33: 561–569.

Dean, T.J. and J.N. Long. 1986. Variation in sapwood area-leaf area relations within two stands of lodgepole pine. For. Sci. 32: 749–758.

Deleuze, C. and F. Houllier. 1995. Prediction of stem profile of *Picea abies* using a process-based tree growth model. Tree Physiol. 15:113–120.

de Pury, D.G.G. and G.D. Farquhar. 1997. Simple scaling of photosynthesis from leaves to canopies without the errors of big-leaf models. Plant Cell Environ. 20:537–557.

Dewar, R.C. and R.E. McMurtrie. 1996. Analytical model of stemwood growth in relation to nitrogen supply. Tree Physiol. 16: 161–171.

Dewar, R.C., B.E. Medlyn and R.E. McMurtrie. 1998. A mechanistic analysis of light and carbon use efficiencies. Plant Cell Environ. 21:573–588.

Dewar, R.C., B.E. Medlyn and R.E. McMurtrie. 1999. Acclimation of the respiration/photosynthesis ratio to temperature: insights from a model. Global Change Biol. 5:615–622.

Dougherty, A.M., R.B. Corotis and A. Segurson. 2003. Design wind speed prediction. J. Struct. Eng-ASCE. 129:1268–1274.

Farquhar, G.D. and S.C. Wong. 1984. An empirical model of stomatal conductance. Aust. J. Plant Physiol. 11:191–210.

Farquhar, G.D., S. von Caemmerer and J.A. Berry. 1980. A biochemical model of photosynthetic CO_2 assimilation in leaves of C3 species. Planta 149:78–90.

Field, C., J. Merino and H.A. Mooney. 1983. Compromises between water-use efficiency and nitrogen-use efficiency in five species of California evergreens. Oecologia 60:384–389.

Gardiner, B., H. Peltola and S. Kellomaki. 2000. Comparison of two models for predicting the critical wind speeds required to damage coniferous trees. Ecol. Model. 129:1–23.

Grote, R. 1998. Integrating dynamic morphological properties into forest growth modeling. II. Allocation and mortality. For. Ecol. Manage. 111:193–210.

Hari, P., E. Nikinmaa and M. Holmberg. 1990. Photosynthesis, transpiration and nutrient uptake in relation to tree structure. *In* Process Modeling of Forest Growth Responses to Environmental Stress. Eds. R.K. Dixon, R.S. Meldahl, G.A. Ruark and W.G. Warren. Timber Press, Portland, OR, pp 41–48.

Hilbert, D.W. and J.F. Reynolds. 1991. A model allocating growth among leaf proteins, shoot structure and root biomass to produce balanced activity. Ann. Bot. 68:417–425.

Hof, J., D. Rideout and D. Binkley. 1990. Carbon fixation in trees as a micro optimization process: an example of combining ecology and economics. Ecol. Econ. 2:243–256.

Johnson, I.R. and J.H.M. Thornley. 1987. A model of shoot:root partitioning with optimal growth. Ann. Bot. 60:133–142.

Jones, H.G. 1992. Plants and microclimate. Cambridge University Press, Cambridge, 428 p.

Kaufmann, M.R. and C.A. Troendle. 1981. The relationship of leaf area and foliage biomass to sapwood conducting area in four subalpine forest tree species. For. Sci. 27:477–482.

King, D.A. 1990. The adaptive significance of tree height. Am. Nat. 135:809–828.

King, D.A. 1993. A model analysis of the influence of root and foliage allocation on forest production and competition between trees. Tree Physiol. 12:119–135.

Le Roux, X., A. Lacointe, A. Escobar-Gutierrez and S. Le Dizes. 2001. Carbon-based models of individual tree growth: a critical appraisal. Ann. For. Sci. 58:469–506.

Litton, C.M. 2002. Above- and belowground carbon allocation in post-fire lodgepole pine forests: effects of tree density and stand age. Department of Botany, University of Wyoming, Laramie, 210 p.

Lo, E., M.W. Zhang, M. Lechowicz, C. Messier, E. Nikinmaa, J. Perttunen and R.P. Sievanen. 2001. Adaptation of the LIGNUM model for simulations of growth and light response in Jack pine. For. Ecol. Manage. 150:279–291.

Luan, J., R.I. Muetzelfeldt and J. Grace. 1996. Hierarchical approach to forest ecosystem simulation. Ecol. Model. 86:37–50.

Magnani, F., M. Mencuccini and J. Grace. 2000. Age-related decline in stand productivity: the role of structural acclimation under hydraulic constraints. Plant Cell Environ. 23:251–263.

Mäkelä, A. 1986. Implications of the pipe model theory on dry matter partitioning and height growth in trees. J. Theor. Biol. 123: 103–120.

Mäkelä, A. 1997. A carbon balance model of growth and self-pruning in trees based on structural relationships. For. Sci. 43:7–24.

Mäkelä, A. 1999. Acclimation in dynamic models based on structural relationships. Funct. Ecol. 13:145–156.

Mäkelä, A. and R.P. Sievanen. 1987. Comparison of two shoot-root partitioning models with respect to substrate utilization and functional balance. Ann. Bot. 59:129–140.

Mayhead, G.J. 1973. Some drag coefficients for British forest trees derived from wind tunnel studies. Agric. Meteorol. 12:123–130.

Miller, J.M., R.J. Williams and G.D. Farquhar. 2001. Carbon isotope discrimination by a sequence of *Eucalyptus* species along a subcontinental rainfall gradient in Australia. Funct. Ecol. 15:222–232.

Mooney, H.A., P.J. Ferrar and R.O. Slatyer. 1978. Photosynthetic capacity and carbon allocation patterns in diverse growth forms of Eucalyptus. Oecologia 36:103–111.

Murty, D., R.E. McMurtrie and M.G. Ryan. 1996. Declining forest productivity in aging forest stands: a modeling analysis of alternative hypotheses. Tree Physiol. 16:187–200.

Nardini, A., S. Salleo and F. Raimondo. 2003. Changes in leaf hydraulic conductance correlate with leaf vein embolism in *Cercis siliquastrum* L. Trees 17:529–534.

Pearson, J.A., T.J. Fahey and D.H. Knight. 1984. Biomass and leaf area in contrasting lodgepole pine forests. Can. J. For. Res. 14: 259–265.

Peltola, H., S. Kellomaki, H. Vaisanen and V.-P. Ikonen. 1999. A mechanistic model for assessing the risk of wind and snow damage to single trees and stands of Scots pine, Norway spruce and birch. Can. J. For. Res. 29:647–661.

Pielou, E.C. 1981. The usefulness of ecological models: a stocktaking. Q. Rev. Biol. 56:17–31.

Reich, P.B., M.B. Walters and T.J. Tabone. 1989. Response of *Ulmus americana* seedlings to varying nitrogen and water status. 2. Water and nitrogen use efficiency. Tree Physiol. 5:173–184.

Reid, C.P.P., G.J. Odegard, J.C. Hokenstrom, W.J. McConnell and W.E. Frayer. 1974. Effects of clearcutting on nutrient cycling in lodgepole pine forests. Colorado State University and United States Forest Service, Fort Collins, 321 p.

Reynolds, J.F. and J.H.M. Thornley. 1982. A shoot:root partitioning model. Ann. Bot. 49:585–597.

Running, S.W. and J.C. Coughlan. 1988. A general model of forest ecosystem processes for regional applications 1. Hydrologic balance, canopy gas exchange and primary production processes. Ecol. Model. 42:125–154.

Ryan, M.G. 1989. Sapwood volume for three subalpine conifers: predictive equations and ecological implications. Can. J. For. Res. 19:1397–1401.

Ryan, M.G. 1991. A simple method for estimating gross carbon budgets for vegetation in forest ecosystems. Tree Physiol. 9:255–266.

Ryan, M.G. and R.H. Waring. 1992. Maintenance respiration and stand development in a subalpine lodgepole pine forest. Ecology 73:2100–2108.

Ryan, M.G., D. Binkley and J. Fownes. 1997. Age-related decline in forest productivity: pattern and process. Adv. Bot. Res. 27: 213–262.

Sack, L., P.J. Melcher, M.A. Zwieniechi and N.M. Holbrook. 2002. The hydraulic conductance of the angiosperm leaf lamina: a comparison of three measurement methods. J. Exp. Bot. 53: 2177–2184.

Sack, L., C.M. Streeter and N.M. Holbrook. 2004. Hydraulic analysis of water flow through leaves of Sugar Maple and Red Oak. Plant Physiol. 134:1824–1833.

Shinozaki, K., K. Yoda, K. Hozumi and T. Kira. 1964*a*. A quantitative analysis of plant form: the pipe model theory. I. Basic analysis. JPN. J. Ecol. 14:97–105.

Shinozaki, K., K. Yoda, K. Hozumi and T. Kira. 1964*b*. A quantitative analysis of plant form: the pipe model theory. II. Further evidence of the theory and its application in forest ecology. JPN. J. Ecol. 14:133–139.

Simiu, E., N.A. Heckert, J.J. Filliben and S.K. Johnson. 2001. Extreme wind load estimates based on the Gumbel distribution of dynamic pressures: an assessment. Struct. Saf. 23:221–229.

Thornley, J.H.M. 1972*a*. A balanced quantitative model for root:shoot ratios in vegetative plants. Ann. Bot. 36:431–441.

Thornley, J.H.M. 1972*b*. A model to describe the partitioning of photosynthate during vegetative growth. Ann. Bot. 33:419–430.

Tilman, D. 1980. A graphical-mechanistic approach to competition and predation. Am. Nat. 116:362–393.

Tilman, D. 1982. Resource competition and community structure. Princeton Monographs in Population Biology. Princeton University Press, Princeton, NJ, 296 p.

Valentine, H. 1985. Tree-growth models: derivations employing the pipe-model theory. J. Theor. Biol. 117:579–585.

Valentine, H. 1999. Estimation of the net primary productivity of even-aged stands with a carbon-allocation model. Ecol. Model. 122:139–149.

Waring, R.H., J.J. Landsberg and M. Williams. 1998. Net primary production of forests: a constant fraction of gross primary production? Tree Physiol. 18:129–134.

Weinstein, D.A., R.M. Beloin and R.D. Yanai. 1991. Modeling changes in red spruce carbon balance and allocation in response to interacting ozone and nutrient stresses. Tree Physiol. 9:127–146.

West, G.B., J.B. Brown and B.J. Enquist. 1999. A general model for the structure and allometry of trees. Nature 400:664–667.

Whitehead, D., W.R.N. Edwards and P.G. Jarvis. 1984. Conducting sapwood area, foliage area and permeability in mature trees of *Picea sitchensis* and *Pinus contorta*. Can. J. For. Res. 14:940–947.

Woodward, F.I. 1987. Climate and plant distribution. Cambridge University Press, Cambridge. 174 p.

Wullschleger, S.D. 1993. Biochemical limitations to carbon assimilation in C3 plants: a retrospective analysis of the A/c_i curves from 109 species. J. Exp. Bot. 44:907–920.

Yoder, B.J., M.G. Ryan, R.H. Waring, A.W. Schoettle and M.R. Kaufmann. 1994. Evidence of reduced photosynthetic rates in old trees. For. Sci. 40:513–527.

Appendix

This Appendix describes the DESPOT (Deducing Emergent Structure and Physiology Of Trees) model. Symbols are defined and units are given in Tables 1 and 2. Figure A1 is a diagrammatic illustration of key structural metrics and of their use in windthrow risk calculations (see *Windthrow risk* below).

Carbon allocation

In each time step, C made available in the previous time step is allocated among three pools (leaf, fine root and sapwood C; C_l, C_r and C_{sw}, respectively) using five allocation fractions—one for leaves (a_l), one for fine roots (a_r), and three for sapwood: radial or diameter growth (a_d), H growth (a_h) and depth (i.e., belowground woody tissue) growth (a_z):

$$a_l \equiv \frac{\delta C_l^+}{\delta C_t^+} \quad a_r \equiv \frac{\delta C_r^+}{\delta C_t^+} \quad a_d \equiv \left(\frac{\delta C_{sw}^+}{\delta C_t^+}\right)_{H,Z}$$
$$a_h \equiv \left(\frac{\delta C_{sw}^+}{\delta C_t^+}\right)_{D_b,Z} \quad a_z \equiv \left(\frac{\delta C_{sw}^+}{\delta C_t^+}\right)_{H,D_b} \tag{A1}$$

where H, Z and D_b are H, depth (i.e., effective length of belowground woody tissue, discussed below under *Structural metrics*) and basal trunk diameter, respectively, C_t is whole-tree C content and the "+" superscripts distinguish new growth from total increments, which include senescence. Senescence and sapwood–heartwood conversion are described below. In each time step, a numerical algorithm identifies the vector of allocation fractions that maximizes single-tree net C gain (A_n)

in the next time step. The total growth increment, δC_t^+, is $A_n \delta t$, where δt is the time step (implicitly 1 year, in the sense that no seasonal effects are considered, but the numerical simulation operates on a much shorter time step of 0.02 years for the sake of stability).

Carbon gain and respiration

Single-tree annual net primary production (A_n) is defined as gross photosynthesis (A_t) minus maintenance respiration (R_m, proportional to tissue N contents) and construction respiration (a fixed fraction (f_c) of $A_t - R_m$):

$$A_n = (1 - f_c)(A_t - R_m) = (1 - f_c)(A_t - v(n_{sw}C_{sw} + n_r C_r + N_t)) \quad \text{(A2)}$$

where v is annual respiration per unit tissue N, n_r and n_{sw} are fine root and sapwood N/C ratios and N_t is total canopy N content. Gross canopy photosynthesis is the product of leaf-level gross photosynthesis and total leaf area (L), upscaled by a time factor, Y:

$$A_t = YL(A + R_l) \quad \text{(A3)}$$

where A and R_l are leaf-level net CO_2 assimilation and daytime respiration rates, respectively. There are three expressions for A. One describes the rate of CO_2 diffusion through stomata, and is denoted A_s (where s = supply-limited):

$$A_s = g_{tc}(c_a - c_i) \quad \text{(A4)}$$

where g_{tc} is total conductance to CO_2 and c_a and c_i are ambient and intercellular CO_2 mole fractions, respectively. When A is limited by CO_2 demand, it approaches the lesser of two values, A_c and A_r, representing RuBP carboxylation and regeneration-limited rates, respectively. A_c and A_r are given by Farquhar et al. (1980) as:

$$A_c = \frac{V_m(c_i - \Gamma_*)}{c_i + K'} - R_l \quad A_r = \frac{J(c_i - \Gamma_*)}{4(c_i + 2\Gamma_*)} - R_l \quad \text{(A5)}$$

where V_m is maximum velocity and K' is effective Michaelis constant for RuBP carboxylation, Γ_* is the photorespiratory compensation point, R_l is daytime leaf respiration rate and J is potential electron transport rate. Both Γ_* and K' are treated as constants; V_m and J are discussed below. Determination of A involves first solving A_s with each of A_c and A_r to constrain c_i and thereby remove it from the equations, and then by calculating the hyperbolic minimum of the two resulting values of A (denoted $A_c \cap A_s$ and $A_r \cap A_s$):

$$A = \text{minh}\{A_c \cap A_s, A_r \cap A_s, \theta_A\} \quad \text{(A6)}$$

where "minh{x,y,z}" is shorthand for "the lesser solution Q of $zQ^2 - (x + y)Q + xy = 0$".

Resource dependence of photosynthetic parameters

Leaf-level transpiration rate (E), nitrogen content (N) and incident photosynthetic irradiance (I) influence g_{tc}, V_m, J and R_l, as follows. The value of J is calculated as minh{J_m, ϕI, θ_J} (Farquhar and Wong 1984); f and θ_J are constants and $J_m = \chi_j N$, and V_m is assumed proportional to J_m as $V_m = J_m/2.1$ (Wullschleger 1993), and R_l is assumed proportional to V_m as $R_l = 0.01V_m$ (de Pury and Farquhar 1997). The value of g_{tc} is given by $g_s/(1.6 + 1.37\, r_{bw}g_s)$, where g_s and r_{bw} are stomatal conductance and boundary layer resistance to water vapor, respectively, and $g_s = E/(D - r_{bw}E)$, where D is leaf-to-air water vapor mole fraction gradient. The leaf-level model for A is assumed scale-invariant (i.e., the canopy is a "big-leaf"), so it is driven by canopy averages for N, I and E: $N = N_t/L$, $I = I_t/L$ and $E = E_t/L$, where L is total leaf area, N_t is canopy photosynthetic N content, E_t is whole-tree transpiration rate, and I_t is canopy absorbed photosynthetic irradiance. The next section describes how E_t, N_t and I_t are calculated.

Photosynthetic resource capture and delivery

Stomatal conductance is calculated from leaf transpiration rate: $g_s = E/(D - r_{bw}E) = E_t/(LD - r_{bw}E_t)$. In turn, E_t is calculated by assuming canopy transpiration occurs in steady-state with uptake by roots and axial flow through coarse roots and the trunk, according to Darcy's Law:

$$E_t = \frac{\Delta P}{r_s + r_x + r_l} = \frac{\psi_s - \psi_l - \rho g h}{(k_{ue}C_r)^{-1} + \frac{l\eta V_w}{k_s S} + \frac{r_{la}}{L}} \quad \text{(A7)}$$

where ρ is water density and g is gravitational acceleration. Vertical distance to the center of the canopy, h (Figure A1c), is $H(1 - 0.5 \cdot \text{LCR}) + Z/\sqrt{2}$, (assuming coarse roots are at a 45° angle), axial flow path length, l (Figure A1b), is $H(1 - 0.5 \cdot \text{LCR}) + Z + 0.5G^{0.5}$) (the last term represents lateral flow parallel to the ground, where G is the ground area subtended by the canopy, or the square of canopy width). Sapwood permeability is k_s, η is dynamic viscosity of water (1.0×10^{-9} MPa s at 20 °C) and V_w is molar volume of water (18×10^{-6} m^3 mol^{-1}). The laminar resistance and total surface area of a single leaf are assumed constant, so r_{la} is also a constant. Soil water potential, (Ψ_s), is treated as a constant. In the present paper, leaf water potential (Ψ_l) is also assumed constant, representing an isohydric state adapted to keep xylem tension above some threshold. The accompanying paper (Buckley and Roberts 2006) relaxes the isohydric assumption to study the effect of dynamic compensation mechanisms (increased sapwood permeability or reduced Ψ_l with H) and the costs of associated increases in embolism risk.

The total amount of N contained in leaves, (N_t), is simulated dynamically as the balance between N sources (uptake by fine roots and inputs of recycled N from senescing tissues) and N sinks other than new leaves (losses due to leaf senescence and N requirements of new fine roots and sapwood). Following Dewar and McMurtrie (1996), we assume N uptake is a fraction of the total rate of inputs into the soil and that the fraction

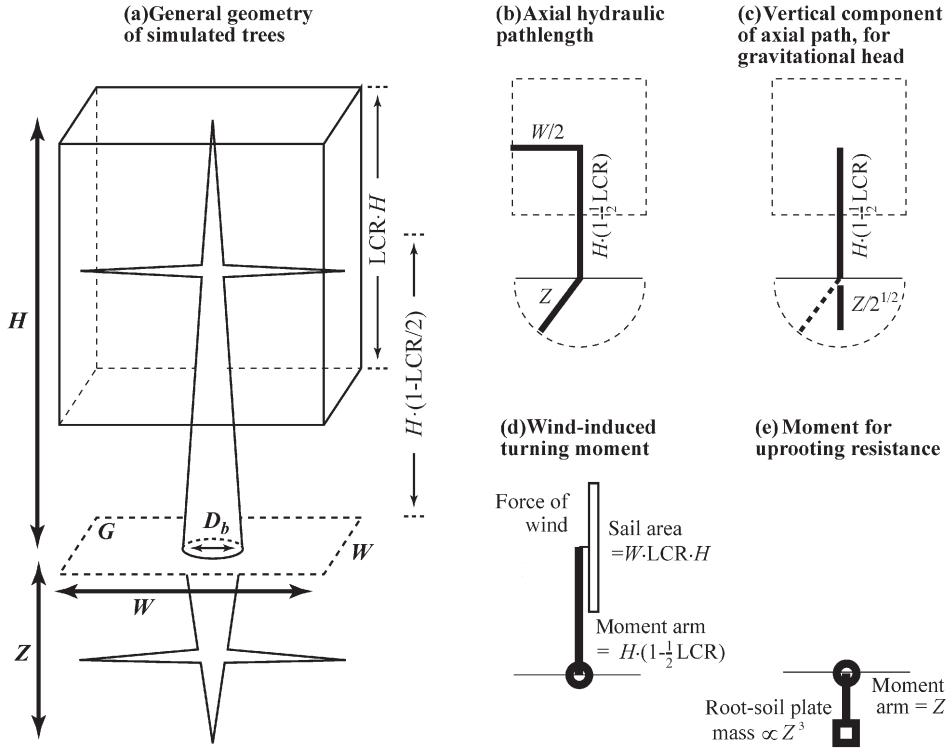

Figure A1. Diagrammatic illustrations of (a) assumed tree geometry in DESPOT and of its relationship to the calculations of (b) axial hydraulic path length (Equation A7), (c) vertical displacement for gravitational hydraulic head (Equation A7), (d) wind-induced turning moment (Equations A22 and A23) and (e) moment for uprooting resistance (Equations A22 and A23). In (a), the 3-dimensional rectangular box represents the canopy and the shaded area below it represents the projected ground area of the canopy (G). Height (H), canopy width ($W = G^{0.5}$), canopy H (LCR·H, where LCR is live crown ratio) and rooting depth (Z) are also indicated in (a). Details about the calculations represented in b–e are given in the Appendix. Abbreviation: D_b = basal trunk diameter.

increases in saturating fashion with fine root C per unit ground area (C_r/G). Then, if N inputs occur at a rate of U_o per unit ground area, the rate of N uptake is:

$$U = (GU_o)\frac{\frac{C_r}{G}}{\frac{C_r}{G}+\kappa} = \frac{GU_oC_r}{C_r+G\kappa} \quad \text{(A8)}$$

where κ is fine root C per ground area at which uptake equals half the input rate. The finite increment in N_t in one time step is then given by:

$$\delta N_t = \left((U+\gamma_l n_l \delta C_l^- + \gamma_{sw} n_{sw} \delta C_{sw}^-) - (n_l \delta C_l^- + n_r \delta C_r^+ + n_{sw} \delta C_{sw}^+)\right)\delta_t \quad \text{(A9)}$$

where λ_l and λ_{sw} are leaf and sapwood N recycling fractions; δC_l^- and δC_{sw}^- are senescence losses of leaf and sapwood C in the current time step; and n_l (leaf N/C ratio) is shorthand for N_t/C_l.

Light capture (I_t) is estimated by analogy to the Beer-Lambert Law. For a laterally uniform canopy with spherical leaf angle distribution and uniform spatial distribution of leaf area, I_t may be approximated as $I_t = GI_s\cos\beta\,(1 - e^{-k/\mathrm{LAI}\sec\beta})$, where I_s is the incoming irradiance on a surface normal to the solar beam and β is the solar elevation below the zenith (Figure A2). This does not, however, predict the increase in light capture resulting from vertical growth that puts some of a tree's canopy above its neighbors. In that case, the change in I_t can be estimated by integrating along each of a series of parallel solar paths, some of which are attenuated by adjacent trees before reaching the "target" tree (Figure A2). Light capture is then equal to $\alpha_c GI_s$, where canopy absorptance, α_c, is:

$$\alpha_c = G^{-0.5}\cos\beta\int_0^{\sqrt{G}} e^{-kp_n(x)}\left(1-e^{-kp_t(x)}\right)dx \quad \text{(A10)}$$

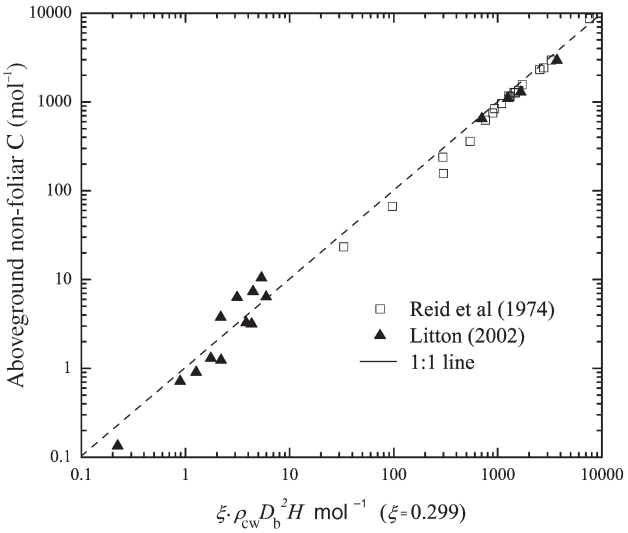

Figure A2. Estimated versus measured aboveground woody carbon, based on measurements of biomass, height (H) and basal diameter (or DBH corrected to basal diameter) made by Reid et al. (1974) (open symbols) and Litton (2002) (closed symbols) for lodgepole pine trees in stands of varying nutrient status and stand densities. The parameter ξ was chosen to produce the best fit. The 1:1 line is shown for comparison. Abbreviations: ρ_{cw} = wood carbon density; and D_b = basal trunk diameter.

where $k = k_L LAI/h$ is an effective extinction coefficient relative to path length, h is canopy depth (LCR·H) and $p_t(x)$ and $p_n(x)$ are the path lengths through the target tree and neighboring trees, respectively, expressed as functions of the horizontal position of each path's intersection with the top of the canopy (Figure A2). It can be shown that this integral evaluates to two different expressions, depending on β. For low β (sun high in the sky) or short or broad trees (β < arctan($\sqrt{G}$/h), Figure A2):

$$\alpha_c = \alpha^o \cos\beta + G^{-0.5}\alpha^+ \left(\alpha^o k^{-1}\cos\beta\sin\beta - (h-\delta H)\sin\beta e^{-k(h-\delta H)\sec\beta}\right) \quad \text{(A11)}$$

where $\alpha^o = 1 - \exp(-kh\sec\beta)$ and $\alpha^+ = 1 - \exp(-k\delta H\sec\beta)$. For high β or taller, narrower trees (β ≥ arctan($\sqrt{G}$/h, Figure A2), α_c is:

$$\alpha_c = \cos\beta\left(1 - e^{-k(h-\delta H)\sec\beta}\right) + G^{-0.5}\,\alpha^+ k^{-1} \cos\beta\sin\beta\left(1 - e^{-2r_c k\sec\beta}\right) \quad \text{(A12)}$$

(When $\delta H = 0$, both expressions for α_c collapse to $\cos\beta(1 - e^{-k_L LAI\sec\beta})$). This formulation is incorrect before canopy closure, because it does not account for open space between adjacent trees. However, although the error overestimates the benefit of H growth before closure, the model predicts negligible H growth before canopy closure, so the effect of the error is also negligible.

Structural metrics

We assume total stem volume is proportional to the product of basal area and the sum of H, Z and $W = G^{1/2}$ (crown width), thus:

$$\text{stem volume} = \xi D_b^2(H + Z + W) = \rho_{cw}^{-1} C_w \quad \text{(A13)}$$

where D_b is basal trunk diameter, $C_w = C_{sw} + C_{hw}$, ρ_{cw} is wood C density and ξ is an empirical parameter relating linear dimensions to wood volume. Although tapering and branching are not explicitly described, ξ implicitly captures the aspects of tapering and branching relevant to DESPOT. The value of ξ used in these simulations (0.299) corresponds to an aboveground woody branching network with about 50% more volume than a single stem of length H and standard −3/2-law taper; this value was found to describe aboveground woody allometry for lodgepole pine across a broad range of tree sizes (Figure A3; see *Parameter estimation* for more details).

Positive increments in stem C occur only by sapwood production, so $\delta C_w^+ = \delta C_{sw}^+$ when calculating allocation. To calculate increments in D_b, S, H and Z given a total available C increment (δC_t), the first step is to deduct from δC_t the cost in stem C of lateral canopy extension to cover ground area freed up by stand thinning. This is done by calculating the change in ground area and thus in W (δW) caused by thinning, from δC_t and the self-thinning equation (Equation A21) and then calculating the increment in C_{sw} needed to produce lateral stem extension of δW, from the product of δW and the sensitivity of C_w to W:

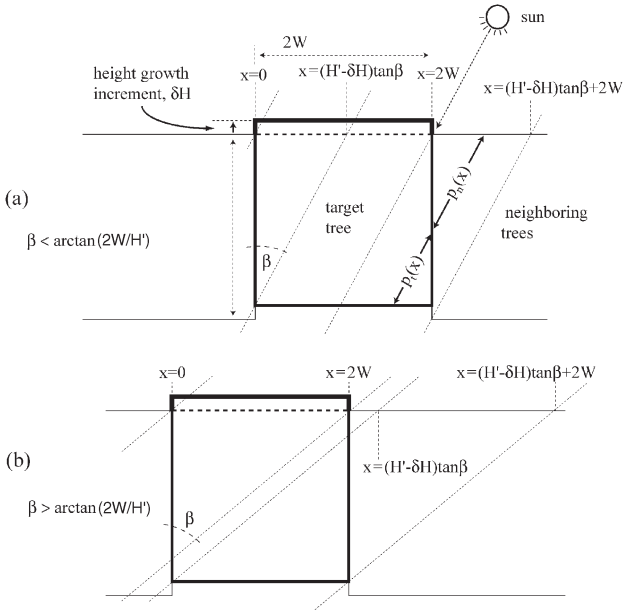

Figure A3. Diagram illustrating the way in which DESPOT calculates the additional light capture that would result from a small vertical growth increment (δH) for a single tree with a box-shaped canopy in a homogeneous stand. Light capture is calculated by integrating along a continuous series of parallel solar paths, each of which may be attenuated before reaching the "target tree," as a result of passing through a neighboring tree's canopy. The light-absorbing path lengths through the neighboring and target trees are $p_n(x)$ and $p_t(x)$, respectively, where x identifies the path by the horizontal position of its intersection with the top of the canopy. Two separate cases must be considered (a and b), depending on whether solar elevation is below the zenith (β) in relation to canopy width to height (H) ratio. Vertical growth increases total light capture by reducing the amount of target canopy receiving any given degree of shade. Abbreviation: W = crown width.

$$\delta C_t' \approx \delta C_t - \delta W\left(\frac{\partial C_w}{\partial W}\right) = \delta C_t - \delta W \cdot \xi\rho_{cw} D_b^2 \quad \text{(A14)}$$

The total C increment available for allocation, $\delta C_t'$, is then partitioned in similar fashion to calculate increments in D_b, H and Z:

$$\delta H = a_h \delta C_t'\left(\frac{\partial H}{\partial C_w}\right) = \frac{a_h \delta C_t'}{\xi\rho_{cw} D_b^2} \quad \text{(A15)}$$

$$\delta Z = a_z \delta C_t'\left(\frac{\partial Z}{\partial C_w}\right) = \frac{a_z \delta C_t'}{\xi\rho_{cw} D_b^2} \quad \text{(A16)}$$

$$\delta D_b = a_d \delta C_t'\left(\frac{\partial D_b}{\partial C_w}\right) = \left(\frac{a_d \delta C_t'}{2\xi\rho_{cw} D_b (H + Z + W)}\right) \quad \text{(A17)}$$

Senescence and heartwood conversion

The processes that determine senescence rates and sapwood to heartwood conversion are not well understood, so we simulate senescence empirically. Each time step's new increment in leaf, fine root and sapwood C is tracked over time and a portion of that increment is deducted in each subsequent time step, based on the increment's age. We found sapwood lifespan distributions in lodgepole pine trees from northwestern Wyoming obeyed a Weibull lifespan distribution with median lifespan 14 years (see *Parameter estimation*); the failure rate (the probability of a randomly chosen increment failing, i.e., senescing) for this type of distribution is $\varepsilon(\text{age}/\text{lifespan})^{\varepsilon-1}$, where ε is a dimensionless parameter. We assumed that leaf and fine root increments had senescence dynamics qualitatively similar to those of sapwood, but with different median lifespans (τ_l and τ_r, respectively).

Thus, in each time step $t \rightarrow t + \delta t$, the increment δC_x^+ produced at each earlier time T (where the subscript x represents sw, l or r, for sapwood, leaves and fine roots, respectively) is decremented such that what remains of the original increment in the next time step, $\delta C_x^+(T; t + \delta t)$, is given by Equation A18:

$$\delta C_x^+(T; t+\delta t) = \delta C_x^+(Tt) - \delta t\, \varepsilon_x \left(\frac{t-T}{\tau_x}\right)^{\varepsilon_x - 1} \qquad \text{(A18)}$$

where the τ_x are tissue-specific median lifespans (τ_s, τ_l or τ_r). The new value of C_x is then calculated by summing the surviving remainders of all previous increments and adding the current time step's new increments (Equation A19):

$$C_x(t+\delta t) = \sum_{T=0}^{t} \delta C_x^+(T;\, t+\delta t) + a_x(t+\delta t)\delta C_t' \qquad \text{(A19)}$$

For sapwood, $a_x = a_h + a_d + a_z$, and the C increment due to lateral crown expansion, calculated from Equation A14, is added to the value of C_{sw} calculated by Equation A19. Heartwood C (C_{hw}) is incremented in each time step by the amount of sapwood C lost in that time step, which is given by $C_{sw}(t)$ minus the term in square brackets on the right-hand side of Equation A19. Sapwood area (S) was calculated from C_{sw} assuming the sapwood/heartwood area fraction was uniform throughout the tree, so that sapwood volume is $S(H + Z + W)$ and:

$$S = \frac{C_{sw}}{\left(\xi \rho_{cw}(H+Z+W)\right)} \qquad \text{(A20)}$$

Stand and environment

Although DESPOT is an individual-tree model, some information about stand properties is required to complete the simulation; for simplicity, we assume the stand consists of identical, evenly spaced trees, and that density-dependent mortality causes stand density (ρ_s) to vary with the −2/3 power of single tree biomass (proportional to total):

$$\rho_s = \rho_{sc} C_t^{-\frac{2}{3}} \qquad \text{(A21)}$$

where ρ_{sc} is a constant. Single tree projected ground area (G) is the lesser of $1/\rho_s$ and projected leaf area, $L_p = L/3.34$ (3.34 converts all-sides to projected area for lodgepole pine (Ryan 1992); a different value should be used for other species.) To calculate single tree light capture, leaf area index (LAI) is L_p/G, which is never less than unity. Note that the value of LAI presented in the figures and in Table 3 is an all-sides, stand-level value ($\rho_s L$).

Penalizing windthrow risk

The model outlined above produces a continuous relationship between allocation parameters and C gain, so it appears economically self-contained. However, it does not impose a cost on windthrow risk, because windthrow does not affect C balance until it causes mortality. We costed tree geometry with respect to windthrow risk by modulating allocation to maximize expected net C gain, based on the probability that a certain tree geometry will fail in severe winds.

The tree will break or uproot if the wind drag (T_w, the turning moment imposed on the stem by wind) exceeds either the bending moment causing stem breakage (T_b) or the turning moment causing uprooting (T_u). These moments may be approximated as follows. Wind at speed v applies a force proportional to v^2 on the canopy, whose "sail area" in calm air is $W(\text{LCR}H)$ ($W = G^{0.5}$ is crown width); supposing the vertical center of this sail is anchored to the stem, the lever arm is $H(1 - 0.5\text{LCR})$. However, canopy streamlining reduces the effective sail area as wind speed rises, such that drag increases roughly linearly with v, rather than v^2 (Mayhead 1973). Hence, we may write $T_w \propto vWH^2\text{LCR}(1 - 0.5\text{LCR})$ (Figure A1d). The critical bending moment causing stem breakage, T_b, is proportional to the cube of basal diameter, D_b^3 (e.g., Jones 1992, Peltola et al. 1999, Gardiner et al. 2000). The HWIND model (Peltola et al. 1999) assumes resistive moment for uprooting is proportional to the mass of the root:soil plate, with lever arm equal to depth of the root:soil plate. We assume the root system occupies a hemispherical volume of radius Z (rooting depth), and that its density is constant so its mass scales isometrically with its volume (Z^3). Hence $T_u \propto Z(Z^3)$ (Figure A1e). Equating T_w with T_b and T_u yields

$$V_b = \frac{w_b D_b^3}{xWH^2} \qquad \text{(A22)}$$

$$V_u = \frac{w_u Z^4}{xWH^2} \qquad \text{(A23)}$$

where V_b and V_u are dimensionless variables proportional to the critical windspeeds for stem breakage and uprooting, respectively, w_u and w_b are empirical parameters and $x = \text{LCR}(1 - 0.5\ \text{LCR})$. This approach is a simplification of some aspects of the more rigorous and flexible HWIND model (Peltola et al. 1999), which requires numerical solution and many parameters. Wind speed frequencies are well described by a

reverse Weibull distribution (Simiu et al. 2001, Dougherty et al. 2003), so the probability p_x that an observation V_x exceeds some value V^* (where x is shorthand for either b or u, representing breakage and uprooting, respectively) is

$$p_x = p(V_x > V^*) = (1 + \omega V_x)^{-\frac{1}{\omega}} \quad \{\omega < 0 \text{ and } 0 < V_x < -\omega^{-1}\} \tag{A24}$$

To apply these windthrow risk calculations to our simulations, A_n first was calculated without consideration of mechanical stability for each C allocation vector in each time step. Then, Equations A22–A24 were used to calculate the annual probabilities of breakage and uprooting, given the values of D, H, Z and G that would result in the next time step from each candidate allocation vector. Finally, A_n was multiplied by the complement of the larger of these two probabilities. The net effect of this procedure is to penalize mechanically risky tree geometries, to make them appear less profitable to the optimization algorithm. Estimation of the parameters w_b, w_u and ω is described under *Parameter estimation*.

Numerical optimization procedures

In each time step, C allocation vectors (sets of C allocation fractions, a_l, a_r, a_d, a_h and a_z, that sum to unity) that maximized A_n in the subsequent time step were identified using a genetic algorithm having the following procedure: (1) $n{\cdot}m$ vectors were generated randomly. (2) A_n was calculated for each vector. (3) The m highest-scoring vectors were identified. (4) Then n new vectors were generated from each of the m winners by mutating the winners' original components (say a_j), by choosing new components randomly in the range $a_j(1 \pm B)$ and renormalizing the resulting vectors. (5) Steps 2–4 were repeated until the square of the relative difference in A_n between the best and the mth best vectors was less than some threshold, δ. To ensure continued improvement between cycles, B was reduced exponentially in successive cycles. In the simulations presented here and in the accompanying paper (Buckley and Roberts 2006), the numerical values of n, m, δ and B were 500, 4, 10^{-15} and 0.5, respectively.

A Nelder-Mead simplex technique worked on simpler versions of this model; we tried a simplex and numerous other hill-climbing and conjugate gradient techniques on DESPOT, but none proved sufficiently robust, even when the search routine was performed in an edgeless space transformed from the hyperplane segment comprising allowable allocation vectors. For any technique to work, we found it necessary to remove all thresholds or slope discontinuities in the model's mathematical structure by hyperbolic minimization or maximization.

Parameter estimation

Most values in the standard parameter set given in Table 2 were estimated for the 40-year-old lodgepole pine stand studied initially by Ryan and Waring (1992) (RW) and later by Yoder et al. (1994) and Murty et al. (1996) (MMR). Parameters that could not be estimated on that basis were taken from the literature or derived from our own measurements of pure lodgepole pine stands in the Shoshone National Forest of Wyoming, USA, in 2000 and 2001.

Parameters taken directly from MMR or RW include leaf and sapwood N recycling efficiencies (γ_l and γ_{sw} = 0.5 and 0.6); median leaf and fine root lifespans (τ_l and τ_r = 8.3 and 1 years); N content of new sapwood (n_{sw} = 1.2 mmol N (mol C)$^{-1}$); canopy light extinction coefficient (k_L = 0.5 m^{2}m^{-2}); leaf area per unit leaf C (SLA = 0.091 m^2 (mol C)$^{-1}$); construction respiration fraction (f_c = 0.22, based on 28% of NPP; RW); self-thinning parameter (ρ_{sc} = 49 stems m^{-2} (mol C)$^{\frac{2}{3}}$; estimated by fitting the self-thinning curve to biomass and stand density data from RW). The following parameters were taken directly from other sources: fine root N:C ratio, n_r = 17mmol N (mol C)$^{-1}$ (Dewar and McMurtrie 1996); N cost of electron transport capacity, χ_j = 1.9 μmol e$^-$ (mmol N)$^{-1}$ s^{-1} (de Pury and Farquhar 1997); annual maintenance respiration per unit tissue N, v = 0.041 mol C mmol^{-1} N year^{-1} (Ryan 1991); wood C density, $\rho_{cw} = 1.4 \times 10^4$ mol C m^{-3}, assuming wood is 40% C by mass (Ryan 1989); sapwood permeability, $k_s = 2.05{\cdot}10^{-12}$ m^2 (Whitehead et al. 1984, for lodgepole pine); and soil and leaf water potential, Ψ_s and Ψ_l = –0.5 and –1.5 MPa (estimated from predawn and midday values given by Yoder et al. 1994 for the 400-year-old RW stand). Laminar resistance (r_{la} = 60 MPa s (mol H_2O)$^{-1}$) was estimated arbitrarily from the low end of the range of values (59–258) found in the literature for broadleaved species (Sack et al. 2002, Nardini et al. 2003, Sack et al. 2004).

The relationship between linear trunk dimensions (D_b, H and Z) and total woody tissue volume (ξ = 0.299 m^{3}m^{-3}; Equation A13) was estimated from allometric data for lodgepole pine (Reid et al. 1974, Litton 2002), from stands with densities ranging from 475–75,500 stems ha^{-1} (plus one plot with nearly 600,000 stems ha^{-1}), with trees of D_b and H ranging from 1–32 cm and 0.6–17.5 m, respectively. Figure A3 shows $\rho_{cw}\xi D_b^2 H$ versus C_w for all of these data, using our values of ξ and ρ_{cw}, and assuming woody biomass was 40% C. This value of ξ corresponds to a branching system where the total volume of aboveground stems and branches is 38% of the volume of a cylinder with basal diameter D_b and length H, or a self-similar, space-filling branching network of length H (both of which have volume = $\pi D_b^2 H/4$): $0.299 D_b^2 H \approx 0.38 (\pi D_b^2 H/4)$. This is roughly 50% more volume than a stem with standard 3/2-law taper (where volume = $\pi D_b^2 H/16$).

Soil-to-xylem hydraulic conductance per unit fine root C ($k_{ue} = 6.6 \times 10^{-4}$ mol H_2O MPa^{-1} s^{-1} mol^{-1}C), was estimated by assuming, arbitrarily, that half the total hydraulic resistance in the 40-year-old RW lodgepole stand occurred in the soil and fine roots; values for axial and total laminar resistance were calculated from H, leaf area and sapwood area in that stand, given our estimates for r_{la} and k_s and assuming belowground axial path was $0.32H$ (from the average ratio of above- to belowground woody biomass in Scots pine and Norway spruce given by Gardiner et al. (2000); those data were also used to estimate windthrow risk parameters below). Nitrogen input (U_o = 660 mmol N m^{-2} year^{-1}) and fine root per ground

area at half uptake saturation (κ = 16 mol C m^{-2}) were estimated assuming N uptake and losses were balanced and uptake was half- saturated in the 40-year-old RW stands.

Median sapwood lifespan (τ_s = 14 years) was estimated from the observed frequency distribution of sapwood lifespans (number of sapwood rings) in 317 lodgepole pine trees from 62 plots in the Shoshone NF, Wyoming in 2001. The number of sapwood rings was calculated from hand measurements of sapwood radius and automated measurements of ring widths on two cores from opposite quadrants of each tree. Live crown ratio (LCR = 0.84) was the average from 27 lodgepole pine trees observed in the Shoshone in 2000 and 2001.

The extreme value index for windspeed frequencies, ω, was taken as –0.25, an approximate value for several Pacific Northwest sites from Dougherty et al. (2003). Values of w_b and w_u were estimated as 1.15×10^5 and 2.3 m^{-1}, respectively; these are average values calculated from data on Scots pine and Norway spruce used by Gardiner et al. (2000) to test the HWIND and GALES models, assuming those observed tree geometries were on the cusp of nonzero probability of damage ($V = -1/\omega = 4$; Equations A22–A24). Boundary layer resistance to water vapor (r_{bw} = 0.5 mol^{-1} m^2 s), leaf-to-air water vapor mole fraction gradient (D = 0.015 mol H_2O mol^{-1}), quantum yield of electrons from incident irradiance (ϕ = 0.3 e^- $photon^{-1}$), and initial stand density (ρ_{si} = 5.0 stems m^{-2} (5000 stems ha^{-1})) were chosen arbitrarily.

Solar beam irradiance (I_s = 1915 μmol m^{-2} s^{-1}) and effective mean solar angle below the zenith (β = 54.5°) were calculated as follows. Incident irradiance on a level surface above the canopy was calculated 20 times in each of 90 days (3 month growing season, June–August), at a latitude of 40° N for the RW sites (using equations given by de Pury and Farquhar 1997), and I_s was adjusted to yield the total growing season PAR given by MMR (converted to photon flux basis assuming λ = 550 nm). Effective mean solar angle was then calculated as the arccosine of the ratio of mean level-surface irradiance over the growing season to I_s.

Total C gain is overestimated when assimilation is extrapolated from the value calculated at a mean irradiance, because assimilation responds to light in saturating fashion. This nonlinear averaging error was corrected by assuming the response of canopy assimilation to irradiance, like that of leaf-level electron transport and assimilation, is described by a non-rectangular hyperbola or "hyperbolic minimum," and by multiplying the number of seconds of daylight in the growing season by the average value (0.67) of the ratio of the hyperbolic minima of actual and mean irradiance over the growing season, using the same convexity parameter (0.90) as for leaf-level J and A. This yields 3.1×10^6 s $year^{-1}$ (0.67 × 90 days × 14.3h × 3600s, where 14.3 h = mean daylength), and hence Y = 3.1 mol $year^{-1}$ (μmol s^{-1})$^{-1}$.